Characterization of Apple Juice Foams for Foam-mat Drying Prepared with Egg White Protein and Methylcellulose

NARINDRA RAHARITSIFA, DIEGO B. GENOVESE, AND CRISTINA RATTI

ABSTRACT: Intrinsic stability and rheological properties of apple juice foams for foam mat drying were studied. Foams were prepared from clarified apple juice by adding various concentrations of 2 foaming agents of different nature: a protein (egg white at 0.5%, 1%, 2%, and 3% w/w) and a polysaccharide (methylcellulose at 0.1%, 0.2%, 0.5%, 1%, and 2% w/w), and whipping at different times (3, 5, and 7 min). In general, egg white foams were less stable but showed a higher degree of solidity (stronger structures), higher foaming capacity, and smaller bubble average diameter than methylcellulose foams. Foam stability increased with increasing concentrations of either methylcellulose or egg white. Increasing whipping times increased the stability of egg white foams only. Stability parameters (maximum drainage and drainage half-time) were correlated in terms of rheological parameters of the continuous phase (consistency index and apparent viscosity at 30/s, respectively). The correlations (R^2 = 0.766 and 0.951, respectively) were considered acceptable because they were independent of whipping time and foaming agent nature and concentration. Results on foam rheology obtained by dynamic and vane tests were in agreement, but the latter method was more sensitive. Optimal concentrations to obtain the most solid foams (0.2% methylcellulose and 2% to 3% egg white, respectively) were the same concentrations required for maximum foaming capacity. Based on this observation and previous models, an empirical expression was proposed to predict the degree of solidity (in terms of inverse phase angle and yield stress) only as a function of foam structural properties (air volume fraction and average bubble size). The model proved to be satisfactory to fit experimental results (R^2 = 0.848 and 0.975, respectively), independently of whipping time, foaming agent nature and concentration.

Keywords: foams, foam-mat drying, stability, rheology, bubbles, continuous phase

Introduction

Foam mat drying involves drying a thin layer of foamed liquid or pureed materials, followed by disintegration of the dried mat to yield a powder. This technique was already applied to dry fruit juices (Hertzendorf and Moshy 1970; Karim and Wai 1999; Vernon-Carter and others 2001), eggs (Satyanarayana-Rao and Murali 1989), and tomato paste (Lovriæ and others 1970). Because of the porous structure of the foamed materials, mass transfer is enhanced leading to shorter dehydration times and consequently, a better quality of the dried products (Brygidyr and others 1977). Although a simple and promising technology, the intrinsic instability of foams has been pointed out as an important problem to be solved before dehydration (Hertzendorf and Moshy 1970; Karim and Wai 1999; Vernon-Carter and others 2001). In addition, foam rheology and structure could help us understand the mechanisms of heat and mass transfer during foam-mat drying. Thus, these aspects of foam characterization deserve to be studied in-depth to properly optimize this process.

Food foams can be considered as biphasic systems in which a gas bubble phase is dispersed in a continuous liquid phase (Herzhaft 1999; Pernell and others 2000; Vernon-Carter and others 2001; Thakur and others 2003). When the volume fraction of gas is high, bubbles are distorted in the form of polyhedra separated by thin liquid films. Three adjacent films intersect in a channel called the Plateau border, and the continuous phase is interconnected through a network of Plateau borders (Narsimhan and Ruckenstein 1986; Narsimhan 1991; Wang and Narsimhan 2004).

Foams are dispersions with a large gas-liquid interface under tension. The manufacture of foams requires an energy input (high-pressure homogenization or whipping) for the expansion of these interfaces. On the other hand, because energy is released under relaxation, foams are inherently unstable (Dickinson and Stainsby 1987; Karim and Wai 1999). The instability process starts with the drainage of the continuous phase through the thin films between the bubbles. As a result, the foam lamellae thins favoring the mass transfer of gas across it, which leads to the growth of large bubbles at the expense of smaller ones (disproportionation or Ostwald ripening). This process continues with bubble coalescence (the thin film between 2 bubbles collapses, and the 2 bubbles merge to form 1 larger bubble), ending in phase separation.

Foam stability is influenced by the physical and rheological properties of the interface and the continuous phase. Foaming capacity and foam stability are enhanced by the adsorption of surface-active molecules (natural or added) at the interface. These surface-active agents form a densely packed layer or film around the bubbles, reducing surface tension and instability (Carp and others 1997; Karim and Wai 1999; Sagis and others 2001; Vernon-Carter and others 2001; Thakur and others 2003). Foams also can be made with macromolecules other than proteins, but only a few polysaccharides, such as modified cellulose derivatives or acetylated pectin are sufficiently active for practical purposes (Dickinson and Stainsby 1987).

The properties of a clarified juice that may affect protein adsorp-

MS 20050554 Submitted 9/14/05, Revised 12/14/05, Accepted 1/24/06. *Authors Raharitsifa and Ratti are with Dept. des Sols et de Génie Agroalimentaire, Faculté des Sciences de l´Agriculture et de l´Alimentation, Univ. Laval, Quebec, Canada. Author Genovese is with Planta Piloto de Ingeniería Química, Camino ¨La Carrindanga¨ Km 7, CC 717, (8000) Bahía Blanca, Argentina. Direct inquiries to author Genovese (E-mail: dgenovese@plapiqui.edu.ar).*

tion to the gas-liquid interface are pH, ionic strength, and sugar content. Foegeding and others (2006) reviewed the main factors determining protein surface activity. Adsorption is generally most rapid at pH values near the protein isoelectric point as electrostatic repulsion is minimized. Accordingly, small amounts of multivalent cations can increase the adsorption of negatively charged proteins via specific electrostatic bridging interactions. The adsorption of ovalbumin was found to decrease in the presence of sucrose, suggesting that ovalbumin participated in hydrogen bonding with the sucrose molecule, increasing its hydrophilicity and hence decreasing its surface activity.

Foaming agents contribute to improve the structure and to control the texture and stability of food foams by modifying the rheological properties of the continuous phase and the interfacial regions where they are adsorbed. Rheological characterization of foams is therefore of primary importance. However, this characterization is a difficult issue, due to the complexity of foam structure. Multiple factors influence the rheology of foams, including air phase volume, liquid phase viscosity, interfacial tension and viscosity, bubble size, size distribution, and shape (Herzhaft 1999; Pernell and others 2000; Vernon-Carter and others 2001; Davis and others 2004). It should be noted that after foam-mat drying, the properties of the rehydrated juice powder could be greatly affected by the foaming additives. For instance, the addition of food stabilizers like xanthan gum and carboxy-methylcellulose dramatically changed the rheological behavior of cloudy apple juice (Genovese and Lozano 2001). Then, the rheological properties of the reconstituted juice and foam's continuous phase might be strongly associated, but this is beyond the scope of this work.

Foams behave as elastic solids at small strains and flow like viscous liquids at large strains (Höhler and others 1999; Vernon-Carter and others 2001). Furthermore, it has been shown that foams exhibit yield stress (Pernell and others 2000; Kampf and others 2003). Yield stress is the minimum stress required to initiate flow (the transition stress from solid-like to liquid-like behavior), and is related to the strength of the network structures of the material (Genovese and Rao 2003). Furthermore, it has been claimed that foam yield stress represents the energy required to pass from 1 stable bubble network to another (Khan and others 1988). Yield stress of foams may be measured by the vane method, which is particularly tolerant to the presence of relatively large bubbles and depletion effects. Overall, the vane geometry has 2 main advantages compared with parallel plates: negligible foam compression during loading (because of its small vertical projected area), and minimization of wall slip effects (produced by foam collapse) (Pernell and others 2000; Genovese and Rao 2003; Davis and others 2004).

The objectives of this work were to (1) analyze the effect of using 2 foaming agents of different nature (polysaccharide and protein) at different concentrations and whipping times, on the stability and physical properties of apple juice foams, (2) predict foam stability in terms of the rheological behavior of the continuous phase, and (3) predict foam rheological behavior in terms of their structural properties (air volume fraction, bubble size, and size distribution).

Materials and Methods

Foam preparation

To prepare fruit juice foams, single-strength clarified apple juice (Del Monte, Nabisco, Ont., Canada) with pH 3.5 was bought in a local market. Methylcellulose (Methocel 65HG, Fluka BioChemika 64670, Buchs Sg, Switzerland) and egg white (Newly Weds, Que., Canada) powders were used as foaming and stabilizing agents. Proper amounts of apple juice and foaming agent were weighed to give final concentrations C of 0.1%, 0.2%, 0.5%, 1%, and 2% (w/w) methylcellulose (MC), and 0.5%, 1%, 2%, and 3% (w/w) egg white (EW). To obtain the foam, the juice was whipped with a kitchen mixer at 3000 rpm while the foaming agent was slowly poured into it, at room temperature. Three different whipping times θ (3, 5, and 7 min) were applied for each concentration. Each sample will be further identified in this work by its concentration, foaming agent, and whipping time. For instance, 05MC3 means 0.5% methylcellulose–3 min whipping, or 1EW7 means 1% egg white–7 min whipping.

Continuous phase preparation

The foams continuous phase was emulated by dissolving each foaming agent in the juice, avoiding foam formation. With that purpose, the right amounts of foaming agent and juice were weighed. The powder was placed in a vessel, small amounts of the juice were gradually added, and the slurry was carefully milled with a mortar until no lumps were observed. Then the rest of the juice was added and gently agitated to homogenize. The resulting solution was subjected to ultrasound under vacuum (10 min) to remove undesired bubbles that could be formed during preparation.

Drainage

A Buchner funnel was filled to the top with 560 mL of each foam. Liquid drained by gravity from the foam was collected in a 250-mL graduated cylinder. The volume of liquid drained V [mL] was measured directly from the graduated cylinder as a function of time during 120 min. The maximum volume of liquid drained V_{max} (final or equilibrium value) was estimated by letting the foam drain overnight and measuring the volume of liquid drained after approximately 20 h.

Rheology of the continuous phase

Flow curves of the continuous phase were obtained by applying a continuous-ramp shear rate in the range 0.02 to 80/s. Measurements were performed in a strain-controlled rheometer (Rheometric Scientific ARES, Piscataway, N.J., U.S.A.) using a Couette geometry (D_{cup} = 34 mm, D_{bob} = 32 mm, L_{bob} = 34 mm). Measurements were done at 20 °C, using the most sensitive transducer.

Rheology of foams

Oscillatory rheological tests. Dynamic rheological data of foams were obtained in the linear viscoelastic range, using a stress-controlled rheometer (Rheometric Scientific SR-5000) with a geometry of parallel plates (40-mm dia, 2.5-mm gap). Frequency sweeps of the elastic modulus G′ and the viscous modulus G″ were obtained at 20 °C. The gap was chosen to be approximately 10 times higher than the average bubble size. Furthermore, a preliminary study showed that at lower gaps, mechanical spectra was affected by plate-plate separation. Same or very similar gaps were used by other authors (Khan and others 1988; Thakur and others 2003) for rheological measurements of foams with parallel plates geometry.

Yield stress tests. Immediately after preparation, part of the foam was gently transferred to a rotating cylinder cup (≈38 mL) attached to a strain-controlled rheometer (Rheometric Scientific). Special care was taken during foam transferring to avoid structure damage and voids. A 4-bladed vane (diameter [D] = 35.72 ± 0.02 mm, height [H] = 11.97 ± 0.01 mm) attached to the rheometer transducer, was completely immersed in the foam. The cup was then rotated at a low constant speed (N = 0.0955 rpm) for 2 min, while the resulting torque produced on the vane-shaft was measured. Yield stress σ_0 was obtained at the point of maximum torque T_m, where the sample flows (Rao 1999):

$$\sigma_0 = T_m \Big/ \left(\frac{\pi D^3}{2} \left(\frac{H}{D} + \frac{1}{3} \right) \right) \quad (1)$$

The procedure was repeated twice by refilling the cup with the original foam, 5 and 10 min after the 1st measurement, respectively. It was found that the time elapsed between measurements had a significant effect on the yield stress measured, which was attributed to foam destabilization and weakening. Consequently, the 2nd and 3rd measurements could not be considered replications of the 1st, but instead used to study the effect of "aging time" Γ on the yield stress of foams.

Air volume fraction

First, foam density ρ_F was determined using the method described by Labelle (1966). Each foam was transferred into a 170 mL (80 mm × 40 mm) brand-crystallizing dish and weighed. Foam transferring was carried out very carefully to avoid destroying its structure or trapping air voids while filling the dish up to 170 mL. Second, the volume fraction of air in each foam sample was calculated with the expression:

$$Ø = 1 - \rho_F/\rho_L \quad (2)$$

where ρ_L is the liquid density (g/cm^3). Eq. 2 is valid if air density is neglected compared with liquid density ρ_L. In this work, juice density was determined to be ρ_L = 1.065 g/cm^3.

Bubble size, size distribution, and shape

Image analysis of foams was performed using a fluorescence microscope Olympus BX51 (Carsen Group Inc., Ont., Canada) with UIS2 optics, which can deliver bright images. A bright-field objective (4X) with U-RSL S plate adapter (phase ring in position 0) and LBD filter was used. Each sample was prepared by placing a suitable amount of fresh foam on a clean glass slide, which was gently pressed down by a cover-slip. An area of 1030 mm × 1300 mm of the cover portion was observed and photographed with a digital camera (CCD) mounted on the microscopy. Image ProPlus imaging software (Media Cybernetics, Silver Spring, Md., U.S.A.) was used to count bubbles and to estimate bubble size and shape parameters. The number of bubbles measured for each size distribution varied with the type and concentration of foaming agent as well as the whipping time, and ranged from 51 to 332 bubbles. To analyze the effect of aging time (Γ), each sample was left to stand in the microscope and subjected to 2 additional measurements, 10 and 20 min after the 1st one, respectively.

Data analysis

All measurements were done at least in duplicate samples, and triplicated when the coefficient of variation was higher than 10%. Nonlinear regression analyses were performed using SigmaPlot software package (Version 8.02, Systat Software Inc., Richmond, Calif., U.S.A.). Data of each foaming agent were subjected to a statistical analysis of variance (ANOVA) using an Excel algorithm, with a significance level of 5%. When necessary, means were compared by the Least Square Difference (LSD) *t*-test.

Results and Discussion

Drainage stability

One way to determine the stability of a foam is to measure the rate at which the liquid drains from it (Kampf and others 2003). The liquid in high-Ø foams is distributed between thin films and Plateau borders. Because of the radius of curvature of a Plateau border, the pressure inside it is less than that in thin films by capillary pressure. This difference, known as Plateau border suction, leads to drainage of liquid from thin films to the neighboring Plateau border. Finally, the liquid in the Plateau border drains under the action of gravity (Narsimhan and Ruckenstein 1986; Narsimhan 1991; Wang and Narsimhan 2004).

Curves of volume of liquid drained as a function of time $V(t)$ followed a sigmoidal shape and were fitted with the equation ($R^2 > 0.980$):

$$V = \frac{V_{max} t^m}{t_{1/2}^m + t^m} \quad (3)$$

where V_{max} is the maximum volume of drained liquid (determined experimentally), m describes the sigmoidal character of the curve, and $t_{1/2}$ is the time required to reach $V_{max}/2$ (drainage half time) (Carp and others 1997). Figure 1a and 1b shows the experimental drainage curves of 5 min whipped EW and MC foams, respectively, fitted with Eq. 3. As expected, drainage decreased at increasing concentrations of both foaming agents. However, the shape of the curves was somehow different. In the case of EW foams, rate of drainage was initially rapid and slowed down at long times, which was characterized by m values close to unity (≈ 1.25). MC foams followed the same trend at low concentrations ($C \leq 0.5\%$). As MC concentration was increased, the shape of the

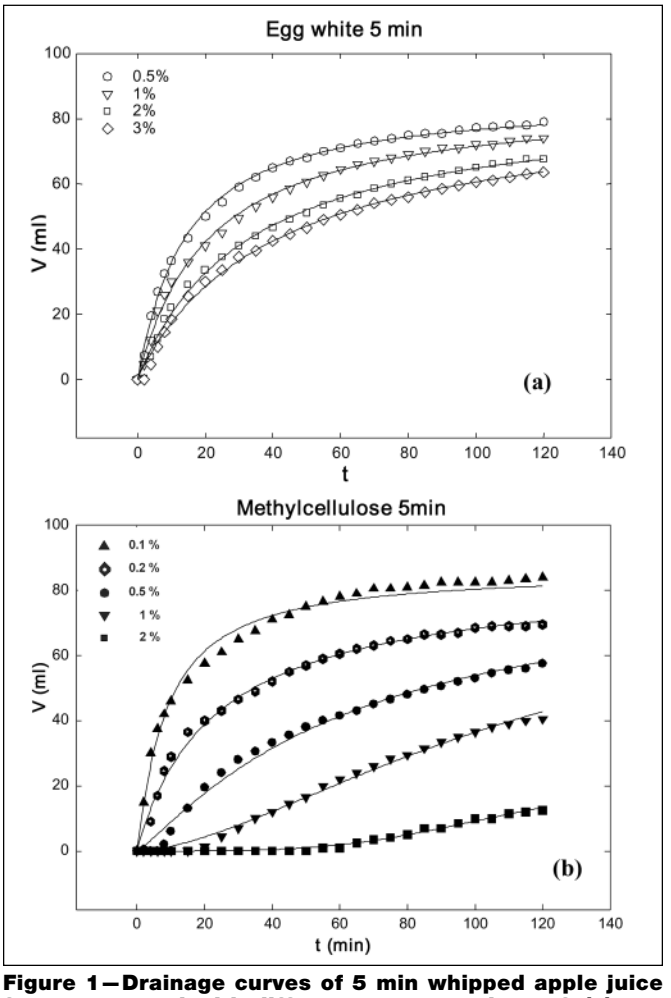

Figure 1—Drainage curves of 5 min whipped apple juice foams prepared with different concentrations of: (a) egg white, and (b) methylcellulose

Table 1—Effect of foaming agent and concentration on the consistency index *K* *100 [Pa.s^n] and the flow behavior index *n* [-] of the continuous phase of apple juice foams[a]

	Methylcellulose *C*%					Egg white *C*%			
	0.1	0.2	0.5	1	2	0.5	1	2	3
K*100	1.75	2.12	2.65	8.39	—	2.06	2.72	4.33	6.60
n	0.674	0.645	0.740	0.892	—	0.546	0.524	0.444	0.378

[a]Calculated by fitting the power law model (Eq. 4) to the flow curves.

drainage curves became more sigmoidal, and *m* values increased up to ≈2.8. This behavior difference could be related to the different foam stabilization mechanisms of EW and MC, as explained later. In addition, the effect of increasing whipping time was to increase *m*: from 1.14 to 1.35 in EW foams, and from 1.27 to 1.73 in MC foams (averaged at all concentrations).

Final foam stability is expected to increase as the maximum volume of drained liquid V_{max} decreases. Consequently, final stability was estimated from maximum drainage, defined as $MD = V_{max}/V_{foam}$, where V_{foam} is the initial volume of the foam (560 mL). Values of *MD* were represented as a function of the concentration of foaming agent (*C*%), at different whipping times (θ) (Figure 2). In general, MC foams showed lower *MD* values (higher final stability) than EW foams. MC foams showed a highly significant decrease of *MD* at increasing *C*, and a significant effect of θ although its trend was not clear.

On the other hand, EW foams showed highly significant interactions between the effects of *C* and θ, meaning that curves followed different trends. However, it can be observed (Figure 2) a general decrease of *MD* at increasing *C*, and also at increasing θ.

Drainage half time $t_{1/2}$ is expected to increase as the drainage rate decrease. Values of $t_{1/2}$ obtained from Eq. 3 were plotted as a function of concentration of foaming agent, at different whipping times (Figure 3). In general, MC foams showed higher $t_{1/2}$ values (lower drainage rates) than egg white foams. Both MC and EW foams showed a highly significantly increase of $t_{1/2}$ at increasing *C*. Similar results were found in soy protein foams (Carp and others 1997). On the other hand, increasing θ produced a highly significant increase on EW foams $t_{1/2}$, but had no significant effect on MC foams $t_{1/2}$.

Overall, increasing concentrations of the foaming agent reduced drainage (increased the stability) of apple juice foams. This may be attributed to an increase in the viscosity and/or yield stress of the continuous phase, and/or to an increase in the thickness and strength of the adsorbed films at the air-water interface (Dickinson and Stainsby 1987; Carp and others 1997; Karim and Wai 1999; Vernon-Carter and others 2001). In this sense, the improved stability of EW foams at increasing whipping times and concentrations may be attributed in part to more protein denaturation and adsorption at the interface, respectively. In spite of this, MC foams were more stable (underwent less drainage) than EW foams, suggesting that foams stability was governed by the rheology of the liquid phase.

Flow curves of the continuous phase of all foams followed shear thinning behavior (no yield stress was observed), and were fitted with the power law model ($R^2 \geq 0.984$):

$$\sigma = K\dot{\gamma}^{n} \quad (4)$$

where σ is the shear stress, *K* is the consistency index, $\dot{\gamma}$ is the shear rate, and *n* is the flow behavior index. It was not possible to obtain flow curves of the 2% MC solution because the bubbles formed in the bulk of the highly viscous liquid could not be removed. For the other solutions, calculated values of *K* and *n* were listed in Table 1.

Values of *K* showed a highly significant increase at increasing either EW or MC concentrations, in agreement with Carp and others (1997). On the other hand, values of *n* showed a highly significant decrease at increasing EW concentrations, but followed the opposite trend for MC. Values of *K* and *n* of MC solutions were higher than values of EW solutions at the same concentrations (0.5% and 1%), probably because MC has a higher molecular weight (300 to 500 kDa) (Keary 2001) than EW (50 to 150 kDa) (Handa and others 2001).

Values of maximum drainage *MD* (averaged at the 3 whipping times) of all foams showed a common trend to decrease with *K* of the

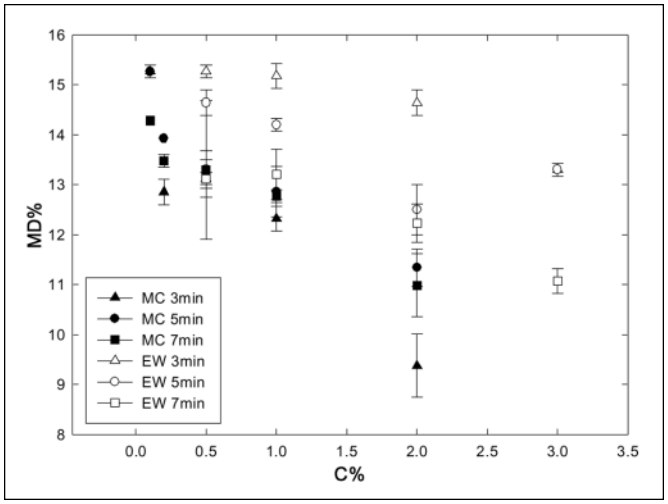

Figure 2—Effect of whipping time and concentration of methylcellulose (MC) and egg white (EW) on the maximum drainage (after 1 d) of apple juice foams

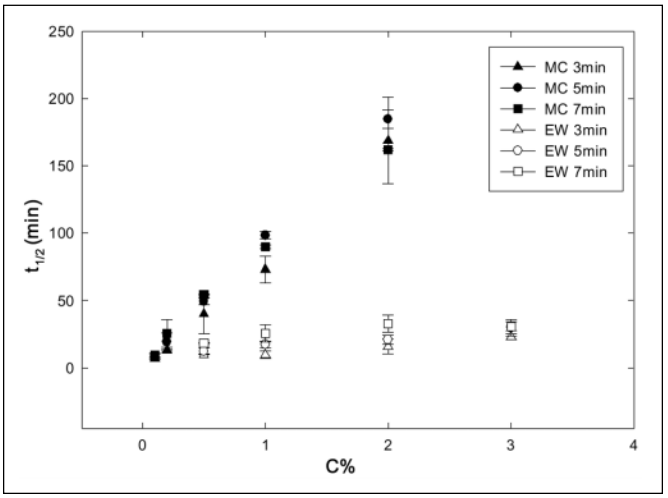

Figure 3—Effect of whipping time and concentration of methylcellulose (MC) and egg white (EW) on the drainage half time of apple juice foams

continuous phase (Figure 4) and were fitted with the equation $MD\% = 12.0 + 4.52/100\ K$ ($R^2 = 0.766$). This correlation was considered acceptable because it is independent of preparation conditions (whipping time and foaming agent nature and concentration). The equilibrium liquid holdup (ϵ_{eq}) is related to MD by the expression $\epsilon_{eq} = 1 - \emptyset_0 - MD$, where $\emptyset_0$ is the initial air volume fraction. The parameter ϵ_{eq} has been modeled (Narsimhan 1991) to be independent of liquid and surface viscosities, which somehow contradicts our results. This discrepancy may be attributed to the fact that Narsimhan's model was developed for ideal dodecahedral bubbles of the same size, whereas foams studied here showed a different bubble geometry (Figure 9 and 10). In addition, Carp and others (1997) found a linear decrease of log k against log K (being $k = m/V_{max}t_{1/2}$, the specific rate constant of drainage), with different slopes for 2 different foams. However, this correlation was not appropriate for the foams studied here.

On the other hand, drainage rate (or drainage velocity) has been established to decrease with increases in the liquid viscosity (Narsimhan 1991; Davis and Foegeding 2004). Foegeding and others (2006) proposed a correlation of the type:

$$t_{1/2} = t_0 + u \cdot \ln(\eta_a) \quad (5)$$

where η_a was the apparent viscosity at a shear rate of 8.5/s (claimed to be chosen within the relevant range of shear rates for liquid drainage and the sensitivity of the rheometer), and t_0 and u are fitting parameters (Davis and Foegeding 2004).

In this work, apparent viscosity was determined from Eq. 4 as $\eta_a = K\dot{\gamma}^{n-1}$, and calculated at different shear rates within the experimental range (10 to 70/s). Figure 5 shows that all foams followed satisfactorily the relationship proposed in Eq. 5, apparently in a common curve. The best correlation ($t_0 = 35.2$ min, $u = 30.7$ min/ln(Pa.s), $R^2 = 0.951$) was obtained with η_a at a shear rate of 30/s. The shear rate at the wall of a Plateau border ($\dot{\gamma}_w$) has been modeled (Wang and Narsimhan 2004) to depend on K, n, and Plateau border radius and drainage driving force.

Rheology

Dynamic rheology. The viscoelasticity of the foams was analyzed in terms of the phase angle, $\delta = arctan(G''/G')$, which varies from 0 for Hookean solids to $\pi/2$ for Newtonian liquids (Steffe 1996). All foams showed a decrease of δ with frequency ω, which was mainly produced by an increase of the elastic modulus G' with ω (not shown), while the viscous modulus G'' remained almost constant. In this context, MC foams followed a behavior somewhere between a concentrated solution and a gel, while EW foams behaved almost like gels. These results are in agreement with previous studies (Khan and others 1988; Thakur and others 2003).

For a better comparison between foams, the phase angle at 1 Hz (δ_{1Hz}) was represented as a function of concentration of foaming agent ($C\%$), at different whipping times (θ) (Figure 6). It can be observed that EW foams showed lower δ_{1Hz} values (higher degree of solidity) than MC foams. EW foams did not show significant variations of δ_{1Hz} with C and θ, giving a global average of $\delta_{1Hz} = 0.227 \pm 0.007$ rad. On the other hand, MC foams showed a general increase of δ_{1Hz} with C, and a highly significant interaction between C and θ.

At this point, it is worth determining the optimal concentration C* of foaming agent that gives the most solid foam (minimum value of phase angle, δ_{Min}). For EW foams, δ_{Min} (averaged at the 3 whipping times) was obtained at C* = 2%, although there were not significant differences with the values obtained at the other C (as previously mentioned).

For MC foams, δ_{Min} was obtained at C* = 0.2%, independently of θ. Phase angle values of MC foams averaged at the 3 whipping times showed no significant differences between δ_{Min} and the values obtained at the neighboring concentrations (0.1% and 0.5%). These results will be later compared with the ones obtained by yield stress measurements.

Vane yield stress. The effect of foaming agent concentration ($C\%$) and aging time (Γ) on the yield stress (σ_0) of foams prepared by 5 min of whipping is represented in Figure 7. It should be noted that no yield stress could be detected on 2% MC foams. In general, EW foams showed higher σ_0 values (stronger structures) than MC foams, in agreement with results obtained by oscillatory tests (Figure 6). Significant and highly significant interactions between the effects of C and Γ were found in EW and MC foams, respectively. Nevertheless, it was found that σ_0 values (averaged at all concentrations) decreased with increasing Γ in both EW and MC foams, suggesting structure weakening produced by destabilization. Furthermore, this effect was less pronounced in MC foams, in agreement with their higher stability showed during drainage measurements. Pernell and

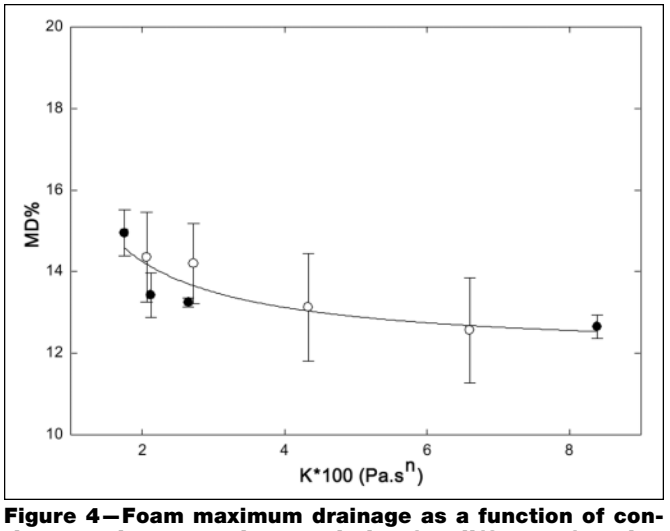

Figure 4—Foam maximum drainage as a function of continuous phase consistency index for different foaming agents: (●) methylcellulose, and (○) egg white. Error bars represent the standard deviation at the 3 whipping times.

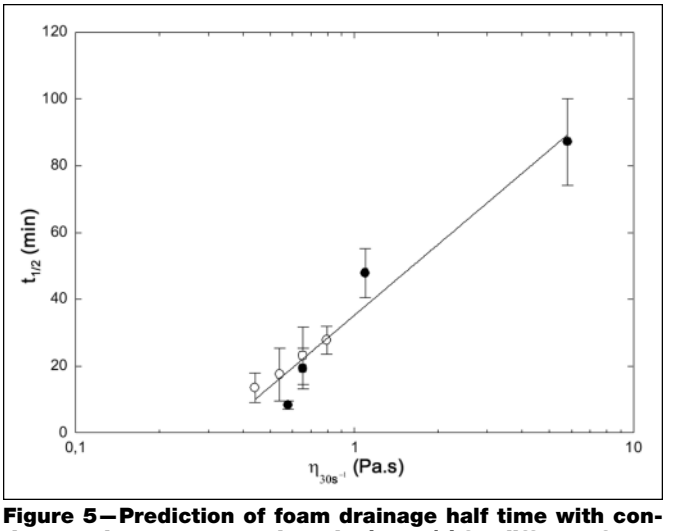

Figure 5—Prediction of foam drainage half time with continuous phase apparent viscosity (at 30/s) for different foaming agents: (●) methylcellulose, and (○) egg white. Error bars represent the standard deviation at the 3 whipping times.

others (2000) also observed that the vane yield stress of protein foams decreased over the time necessary to take 3 measurements.

The optimal concentration C* of foaming agent to obtain the foam with the strongest structure was determined at the maximum yield stress value ($\sigma_{0\text{-}Max}$). For MC foams, $\sigma_{0\text{-}Max}$ was obtained at C* = 0.2%, independently of Γ. In the case of EW foams, C* depended on Γ considered: 3% EW gave the strongest foam initially, but 2% gave the strongest foam after 5 and 10 min. This anomaly was produced by an increase in the yield stress of the 2% EW foam during the 1st 5 min, which was attributed to some systematic experimental error. Yield stress values of each foaming agent were separately averaged at the 3 aging times to analyze the effect of *C*. For MC foams, it was found that yield stress at 0.2% was significantly higher than the values at other *C*. In the case of EW foams, there were not significant differences between the yield stresses at 2% and 3%, but these values were significantly higher than the yield stresses at other *C*.

Overall, results obtained with the vane method were in agreement with the ones obtained by dynamic rheology. However, the vane method found significant differences between C* and the other concentrations, which was not possible with dynamic rheology. This means that vane yield stress is a more sensitive method to determine C*.

The different rheological behavior of EW and MC foams will be explained in terms of their structural properties (air volume fraction and bubble size) later in this work.

Air volume fraction. The volume fraction of gas is a measure of foam quality (Herzhaft 1999). Air volume fraction Ø was represented as a function of concentration of foaming agent (*C*%), at different whipping times (θ) (Figure 8). It can be observed that MC foams showed a general decrease of Ø at $C > 0.5\%$, with a highly significant interaction between *C* and θ. In that range ($C > 0.5\%$), air volume fractions of EW foams were higher than those of MC foams, suggesting higher foaming capacity. Although statistical analysis of EW foams indicated that the effect of *C* on Ø was highly significant, it was negligible compared with the effect observed in MC foams (Figure 8). On the other hand, the effect of θ on Ø was not significant in EW foams.

Density follows exactly the opposite trend than air volume fraction (see Eq. 2). Karim and Wai (1999) found that the density of starfruit puree foams decreased with MC concentrations lower than 0.4% because of a reduction in surface and interfacial tension, but increased at concentrations higher than 0.4% because of an increase in the viscosity of the liquid phase, which would prevent the trapping of air during mixing. Brygidyr and others (1977) found that density of tomato paste foams decreased with whipping time up to a minimum, and increased thereafter probably because of destruction of the foam structure (overbeating). They also found a nonsignificant decrease of density at concentrations of foaming agent higher than 1%.

The optimal concentration C* of foaming agent to achieve maximum foaming was determined at the maximum value of air volume fraction ($Ø_{Max}$).

For EW foams, $Ø_{Max}$ (averaged at the 3 whipping times) was obtained at C* = 2% and was significantly different than the values obtained at the other *C*, except 3%. For MC foams, $Ø_{Max}$ was obtained at C* = 0.2%, independently of whipping time. Air volume fractions of MC foams averaged at the 3 whipping times showed no significant differences between $Ø_{Max}$ and the values obtained at the neighbor concentrations (0.1% and 0.5%). These optimal concentrations values are equivalent to those determined (by dynamic rheology and vane yield stress) for the foams having the strongest structures. The effect of air volume fraction on the strength of foams structure will be analyzed later in this work.

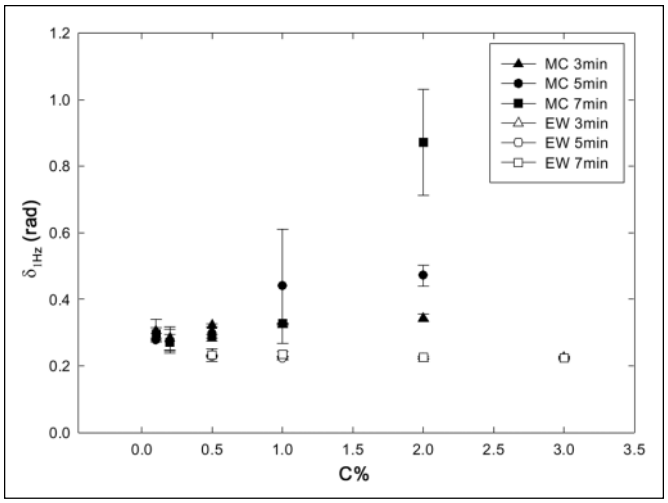

Figure 6—Effect of whipping time and concentration of methylcellulose (MC) and egg white (EW) on the phase angle (at 1 Hz) of apple juice foams

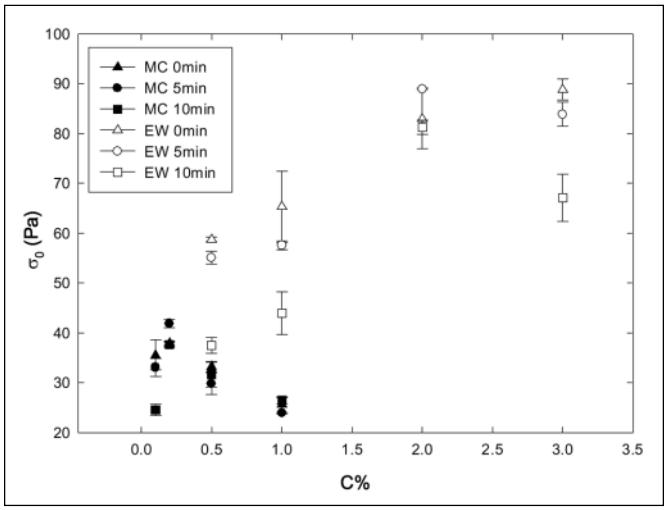

Figure 7—Effect of aging time and concentration of methylcellulose (MC) and egg white (EW) on the yield stress of 5 min whipped apple juice foams

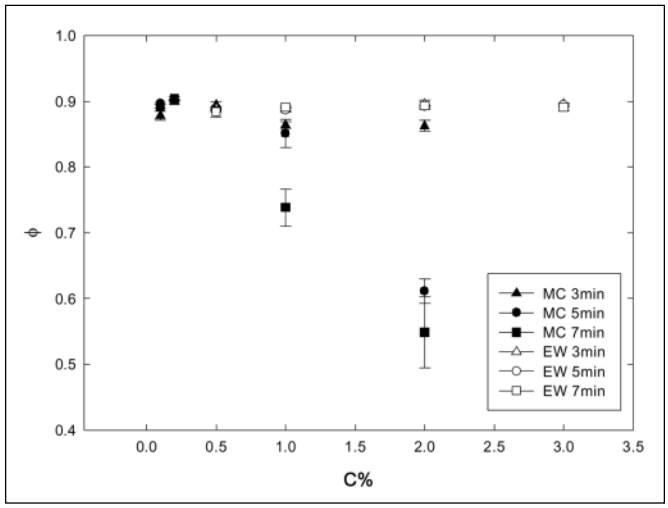

Figure 8—Effect of whipping time and concentration of methylcellulose (MC) and egg white (EW) on the air volume fraction of apple juice foams

When air volume fraction of foams exceeds that of the close-packed-spheres configuration ($Ø_0$) the spherical bubbles are deformed against their neighbors, and as Ø approaches unity the bubbles acquire an increasingly pronounced polyhedral shape. These are called "dry" foams ($Ø > Ø_0$), as opposed to "wet" foams ($Ø < Ø_0$) where the liquid phase volume fraction is high (Princen and Kiss 1989; Carp and others 1997; Herzhaft 1999; Davis and others 2004). All the foams studied in this work except 1MC7, 2MC5, and 2MC7 had air volume fractions (Figure 8) higher than $Ø_0$ of monodisperse systems (≈0.74) and unimodal polydisperse systems (≈0.72). This means that only 3 formulations of MC at high concentrations and high whipping times (1MC7, 2MC5, 2MC7) formed wet foams. All the other formulations of MC and EW in all cases formed dry foams. The effect of air volume fraction on bubble shape is analyzed in next section.

Bubble shape, size, and size distribution

The shape of bubbles below and above the close-packing air volume fraction ($Ø_0$) was visualized in microscopy images of wet and dry foams, respectively. Figure 9 shows 2 foams prepared with the same whipping time but different MC concentrations. At the highest concentration (2MC7), a wet foam was obtained ($Ø < Ø_0$), which showed spherical bubbles (Figure 9a). At the lowest concentration (02MC7), a dry foam was obtained ($Ø > Ø_0$), where crowding produced deformation of bubbles giving them a more polyhedral shape (Figure 9b).

This last effect was always observed in EW foams because all of them were dry foams, as shown in Figure 10a for sample 2EW7. It should be noted that foam 1MC7, which was near the close-packing volume fraction ($Ø \approx 0.74$), did not show bubble deformation (Figure 10b).

To determine a characteristic bubble diameter of each foam, it was considered that foam rheology is affected by the Sauter mean bubble diameter D_{32} (Princen and Kiss 1989; Thakur and others 2003; Davis and others 2004) or surface basis average diameter, which for spherical bubbles is as folllows:

$$D_{32} = \sum d_i^3 \Big/ \sum d_i^2 = 6 \sum V_i \Big/ \sum S_i \qquad (6)$$

where d_i, V_i, and S_i are the diameter, volume, and surface area of each bubble, respectively, and i varies from 1 to the number of bubbles observed.

In this work, the Sauter diameter was calculated from the bubble size distribution on surface basis, considering that bubbles were approximately spherical. Bubbles found in both MC and EW foams were in the range of 0 to 450 mm. This range was divided into 50-mm intervals ($D_j - D_{j-1}$, j = 1 to 9). The average diameter of each interval was calculated as follows:

$$\overline{D}_j = \frac{D_{j-1} + D_j}{2} \qquad (7)$$

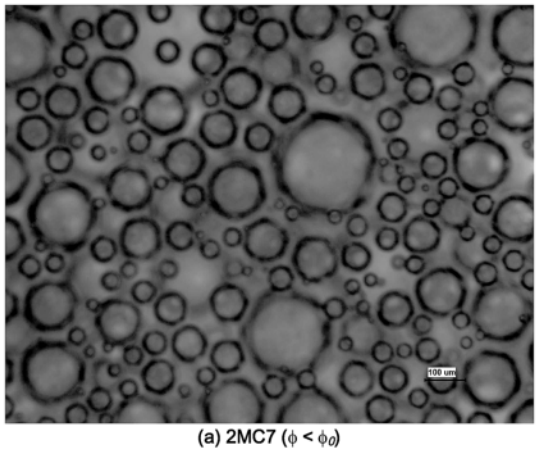

(a) 2MC7 ($\phi < \phi_0$)

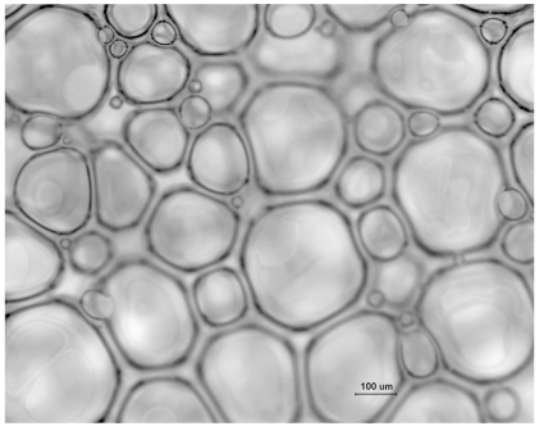

(b) 02MC7 ($\phi > \phi_0$)

Figure 9—Effect of air volume fraction on bubble shape of 7 min whipped apple juice foams at different methylcellulose concentrations: (a) 2% (w/w) and (b) 0.2% (w/w).

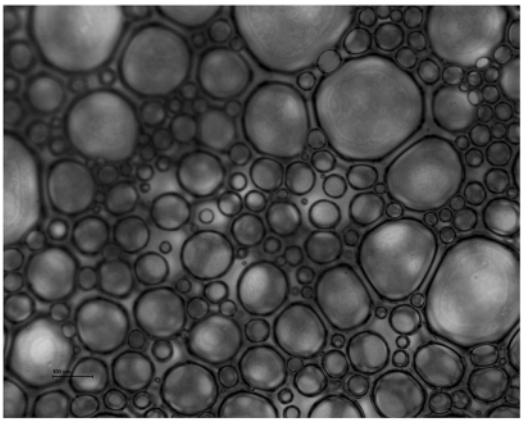

(a) 2EW7 ($\phi > \phi_0$)

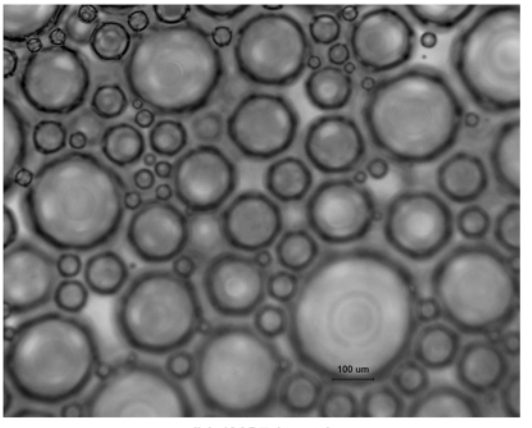

(b) 1MC7 ($\phi \approx \phi_0$)

Figure 10—Effect of air volume fraction on bubble shape of 7 min whipped apple juice foams prepared with (a) 2% egg white and (b) 1% methylcellulose

Table 2—Polydispersity *P* (mm) of bubble size distributions of apple juice foams: effect of whipping time (θ) and foaming agent concentration (C%)[a]

	Methylcellulose *C%*					Egg white *C%*			
θ (min)	0.1	0.2	0.5	1	2	0.5	1	2	3
3	77.7	71.3	72.7	80.4	67.7	55.4	65.8	79.8	59.5
5	82.7	90.9	80.0	73.8	49.5	81.4	80.6	61.6	54.6
7	94.6	73.5	74.7	69.0	54.5	79.8	90.5	69.1	50.7

[a]Calculated values from Eq. 10.

The surface fraction of bubbles in each interval was determined as follows:

$$s_j = \frac{\sum_{D_{j-1}}^{D_j} d_i^2}{\sum d_i^2} \tag{8}$$

Finally, the surface basis average diameter was calculated as follows:

$$D_{32} = \sum s_j \overline{D}_j \tag{9}$$

Values of D_{32} were represented as a function of concentration of foaming agent (*C%*), at different whipping times (θ) (Figure 11). In general, bubble sizes of MC foams (except at 2%) were higher than those of EW foams. In MC foams, values of D_{32} showed a highly significant variation with *C* (increased up to 0.2% and decreased thereafter), and a highly significant decrease with θ.

In EW foams, values of D_{32} showed a significant decrease with *C* and with θ. Karim and Wai (1999) found that bubble average diameter (number basis) increased at concentrations up to 0.4%, and decreased thereafter. Kampf and others (2003) reported that bubble size progressively decreased with whipping time, but Brygidyr and others (1977) found that after reaching a minimum the size increased again because of overbeating. Thakur and others (2003) explained that the minimum bubble diameter corresponds to an equilibrium between viscous forces that tend to disrupt bubbles, and interfacial forces that oppose to bubble break-up.

Polydispersity *P* of bubble size distributions was characterized by their standard deviation:

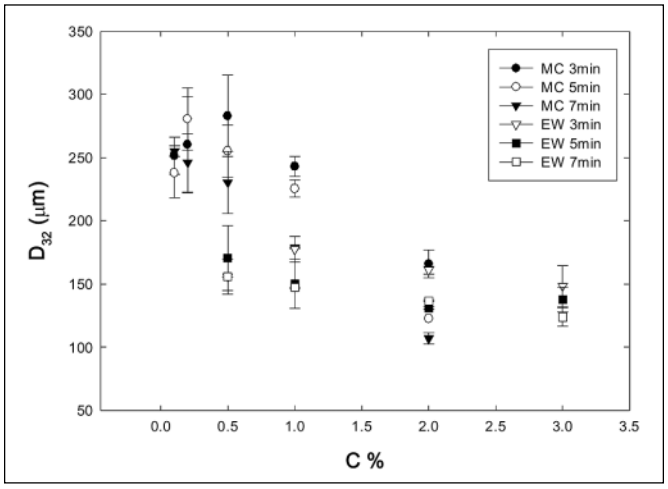

Figure 11—Effect of whipping time and concentration of methylcellulose (MC) and egg white (EW) on the mean (Sauter) bubble diameter of apple juice foams

$$p = \sqrt{\sum s_j \left(D_j - D_{32}\right)^2} \tag{10}$$

For both MC and EW foams, calculated values of *P* ranged approximately from 50 to 95 mm (Table 2), and showed an average decrease at increasing *C*. In contrast, Karim and Wai reported that bubble size distributions were more spread (higher *P* values) and approached a normal distribution at increasing concentrations of MC. On the other hand, increasing θ produced an average increase of *P* in EW foams, but had no effect on MC foams. In contrast, Kampf and others (2003) found that longer whipping times narrowed the bubble size distribution (lower *P* values).

Nevertheless, it has been claimed (Herzhaft 1999) that foam texture is given by gas bubbles size distribution. The global average *P* of EW foams (69.1 mm) was slightly lower than in MC foams (74.2 mm), which may have contributed to the stronger structure of the formers. The effect of bubble size and size distribution on the strength of foams structure will be analyzed in next section.

Finally, all foams showed an "approximately linear" increase of the average bubble size during the first 20 min of observation (not shown). Bubble coalescence was observed only in 3 of 69 micrographs analyzed, and even in those 3 cases it was an isolated phenomenon. Consequently, bubble size growth was attributed to the Ostwald ripening (disproportionation) effect: pressure inside little bubbles is greater than pressure inside big bubbles, then gas diffuse from small bubbles to large bubbles, changing distribution of sizes (Herzhaft 1999; Sagis and others 2001).

Disproportionation effect is clearly visualized in Figure 12 (sample 05E5), where it can be observed how small particles became smaller and large particles became larger after 20 min of aging. To quantitatively compare this effect between the different foams, experimental values were fitted with the following equation:

$$D_{32}/D_{32}^{0} = 1 + k\Gamma \tag{11}$$

where Γ is the aging time after the 1st measurement, D_{32} is the Sauter mean bubble diameter at any Γ (between 0 and 20 min), $D_{32}{}^{\circ}$ is the initial value (at Γ = 0), and *k* is the kinetic constant of bubble size growth. All calculated values of *k* were positive (confirming the increase of bubble size in all foams), and ranged approximately from 5×10^{-3}/min to 2×10^{-2}/min in EW foams, and from 1×10^{-3}/min to 2×10^{-2}/min in MC foams, with an exceptionally high value for sample 2M7 (Table 3). Values of *k* did not show clear trends with *C* nor θ. However, the average *k* value of MC foams (8.84×10^{-3}/min) was lower than the value of EW foams (9.80×10^{-3}/min), confirming that MC foams were more stable, as previously observed from drainage results. It should be noted that some experimental error was introduced by convective movement of the bubbles, not only in the horizontal plane but also between adjacent layers. Höhler and others (1999) reported that bubble radius of shaving foams followed a parabolic growth with aging time (1 h) and attributed it to the Os-

Table 3—Kinetic constant of bubble size growth *k* *100 [/min] in apple juice foams: effect of whipping time (θ) and foaming agent concentration (C%)[a]

	Methylcellulose C%					Egg white C%			
θ (min)	**0.1**	**0.2**	**0.5**	**1**	**2**	**0.5**	**1**	**2**	**3**
3	0.56	0.51	1.73	0.40	0.13	0.96	0.45	1.49	1.26
5	1.61	0.98	0.68	0.27	1.07	1.90	0.80	1.52	0.65
7	0.06	0.18	0.40	0.89	3.82	0.99	0.80	0.47	0.48

[a]Calculated from fitting Eq. 11.

twald effect because bubble coalescence was negligible during that interval.

Predictive model

Because of bubble crowding, when foams with $\emptyset > \emptyset_0$ are subjected to shear deformation at vanishingly small rates, they behave as purely elastic solids (characterized by a static shear modulus, G) up to a yield stress σ_0 above which flow is initiated. Several models have been established for the dependence of G and σ_0 on the relevant physical parameters, that is volume fraction Ø, interfacial tension τ, and the surface basis or Sauter mean bubble diameter D_{32} (Princen and Kiss 1989; Höhler and others 1999; Davis and others 2004).

Based on those models, a simple expression was proposed in this work to predict the degree of solidity DS (either as the inverse phase angle δ^{-1}, or as the yield stress σ_0) of apple juice foams as a function of Ø and D_{32}:

$$DS = a\frac{\phi^{b}}{D_{32}^{c}} \tag{12}$$

where a, b, and c are fitting parameters. Parameter a is expected to include the effect of interfacial tension (not determined in this work).

Values of δ^{-1} (Ø, D_{32}) of all the foams (27 experimental points including both foaming agents) were correlated with Eq. 12 (Figure 13). Resulting regression parameters were as follows: a = 2.48, b = 2.53, and c = 0.445 (R^2 = 0.848). This fit is considered to be satisfactory because Eq. 12 depends only on the structural properties of the foams, and it is independent of preparation conditions (whipping time and foaming agent nature and concentration). It should be noted that the effect of bubble size polydispersity on δ^{-1} was found to be not significant. The same correlation (Eq. 12) was applied to σ_0 (Ø, D_{32}) values of the foams whipped during 5 min (Figure 14). Resulting regression parameters were as follows: a = 18.9, b = 10.9, and c = 1.37 (R^2 = 0.975). It should be pointed out that this regression could have been better than the previous 1 because only 8 experimental points were fitted.

Nevertheless, both parameters showed the same trend: solidity of the foams increased at increasing air volume fractions and at

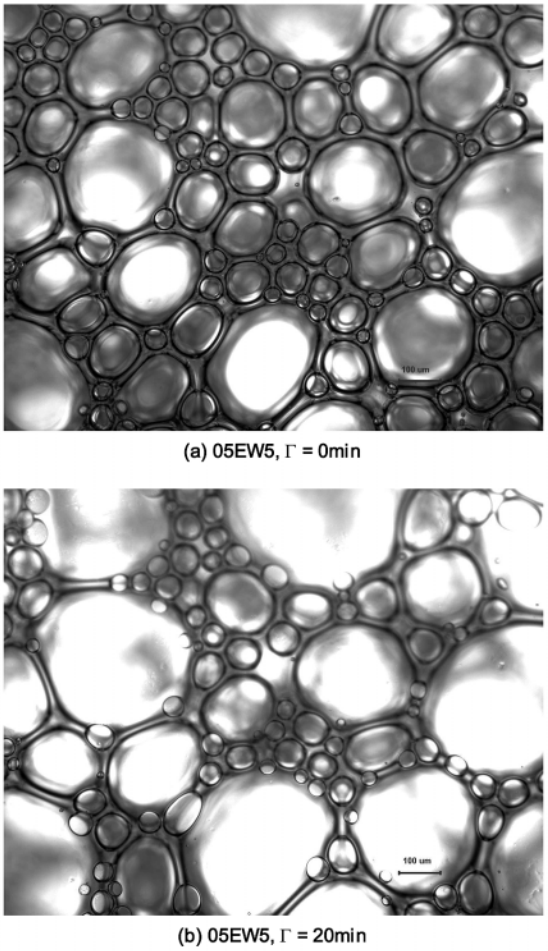

Figure 12—Ostwald ripening effect on bubble size distribution of 5 min whipped apple juice foam prepared with 0.5% EW, at different aging times: (a) 0 min, (b) 20 min

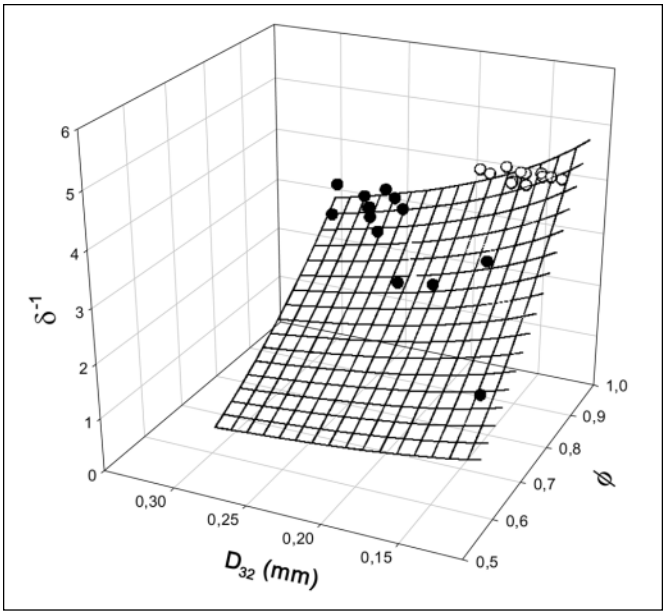

Figure 13—Prediction of apple juice foams degree of solidity (inverse phase angle) with their structural parameters (air volume fraction and bubble mean diameter) for different foaming agents: (●) methylcellulose, and (○) egg white

decreasing bubble sizes. Khan and others (1988) explained that yield stress increased at increasing air volume fractions because foam bubbles become more polyhedral in structure, and consequently larger stresses are required for the bubbles to hop past each another. However, they reported that the ratio G'/G'' does not change with Ø in the range 0.92 to 0.97.

Conclusions

In general, EW foams were less stable but showed a higher degree of solidity (stronger structures), higher foaming capacity, and smaller bubbles than MC foams. Foam stability increased with concentration of foaming agent and was governed by the rheology of the continuous phase. Foams rheology results obtained by the vane method were equivalent, but more sensitive than those obtained by traditional dynamic rheology. Foams with the highest degree of solidity were 0.2% MC and 2% to 3% EW, respectively. It was demonstrated that the degree of solidity of the foams could be predicted from its structural properties (air volume fraction and average bubble size), independently of its formulation and preparation method. Further experimental studies are being conducted on mixed EW-MC foams to find a formulation having the structural properties of EW foams and the stability of MC foams.

Acknowledgments

This work has be.en financially supported by FQRNT (Fonds québecois de la recherche sur la nature et les technologies). Author Genovese is grateful for financial support from CONICET, Argentina, and the Ministère de l'Éducation du Québec, Canada. We thank MS. Mónica Araya for her help with experimental work and valuable discussions.

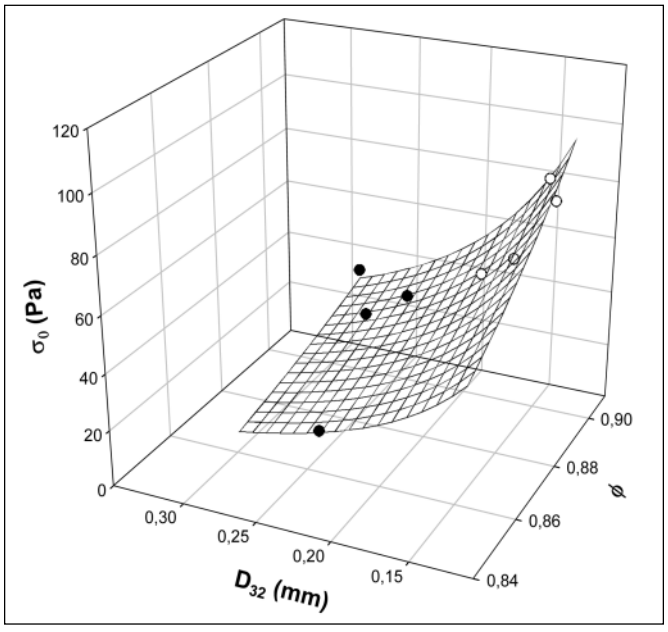

Figure 14—Prediction of apple juice foams degree of solidity (yield stress) with their structural parameters (air volume fraction and bubble mean diameter) for different foaming agents: (●) methylcellulose, and (○) egg white

References

Brygidyr AM, Rzepecka MA, McConnell MB. 1977. Characterization and drying of tomato paste foam by hot air and microwave energy. J Inst Can Sci Technol Aliment 10:313–9.
Carp DJ, Bartholomai GB, Pilosof AMR. 1997. A kinetic model to describe liquid drainage from soy protein foams over an extensive protein concentration range. Lebensm Wiss Technol 30:253–8.
Davis JP, Foegeding EA. 2004. Foaming and interfacial properties of polymerized whey protein isolate. J Food Sci 69:C404–10.
Davis JP, Foegeding EA, Hansen FK. 2004. Electrostatic effects on the yield stress of whey protein isolate foams. Coll Surf B: Biointerf 34:13–23.
Dickinson E, Stainsby G. 1987. Progress in the formulation of food emulsions and foams. Food Technol 41:74–81, 116.
Foegeding EA, Luck PJ, Davis JP. 2006. Factors determining the physical properties of protein foams. Food Hydrocoll 20:284–92.
Genovese DB, Rao MA. 2003. Vane yield stress of starch dispersions. J Food Sci 68:2295–301.
Genovese DB, Lozano JE. 2001. The effect of hydrocolloids on the stability and viscosity of cloudy apple juices. Food Hydrocoll 15:1–7.
Handa A, Hayashi K, Shidara H, Kuroda N. 2001. Correlation of the protein structure and gelling properties in dried egg white products. J Agric Food Chem 49:3957–64.
Hertzendorf MS, Moshy RJ. 1970. Foam mat drying in the food industry. CRC Crit Rev Food Technol 1:25–70.
Herzhaft B. 1999. Rheology of aqueous foams: a literature review of some experimental works. Oil Gas Sci Technol 54:587–96.
Höhler R, Cohen-Addad S, Asnacios A. 1999. Rheological memory effect in aqueous foams. Europhys Lett 48:93–8.
Kampf N, Gonzalez MC, Corradini MG, Peleg M. 2003. Effect of two gums on the development, rheological properties and stability of egg albumen foams. Rheol Acta 42:259–68.
Karim AA, Wai CC. 1999. Characteristics of foam prepared from starfruit (*Averrhoa carambola* L.) puree by using methylcellulose. Food Hydrocoll 13:203–10.
Keary CM. 2001. Characterization of methylcellulose cellulose ethers by aqueous SEC with multiple detectors. Carbohydr Polym 45:293–303.
Khan SA, Schnepper CA, Armstrong RC. 1988. Foam rheology: III. Measurement of shear flow properties. J Rheol 32:69–92.
LaBelle RL. 1966. Characterization of foams for foam mat drying. Food Technol 20:89–114.
Lovriæ T, Sablek Z, Boskovic M. 1970. *Cis-Trans* isomerisation of lycopene and color stability of foam-mat dried tomato powder during storage. J Sci Food Agric 21:641–7.
Narsimhan G. 1991. A model for unsteady state drainage of a static foam. J Food Eng 14:139–65.
Narsimhan G, Ruckenstein E. 1986. Hydrodynamics, enrichment, and collapse in foams. Langmuir 2:230–8.
Pernell CW, Foegeding EA, Daubert CR. 2000. Measurement of the yield stress of protein foams by vane rheometry. J Food Sci 65:110–4.
Princen HM, Kiss AD. 1989. Rheology of foams and highly concentrated emulsions. J Coll Interf Sci 128:176–87.
Rao MA. 1999. Measurement of flow and viscoelastic properties. In: Rao MA, editor. Rheology of fluid and semisolid foods. 1st ed. Gaithersburg, Md.: Aspen Publishers. p 59–151.
Sagis LMC, de Groot-Mostert AEA, Prins A, Van der Linden E. 2001. Effect of copper ions on the drainage stability of foams prepared from egg white. Coll Surf A 180:163–72.
Satyanarayana Rao TS, Murali HS. 1989. Changes in lipids of spray-dried, freeze-dried and foam-mat dried, whole egg powders during storage. Lebensm Wissen Technol 22:217–21.
Steffe JF. 1996. Viscoelasticity. In: Steffe JF, editor. Rheological methods in food process engineering. 2nd ed. East Lancing, Mich.: Freeman Press. p 294–349.
Thakur RK, Vial C, Djelveh G. 2003. Influence of operating conditions and impeller design on the continuous manufacturing of food foams. J Food Eng 60:9–20.
Vernon-Carter EJ, Espinosa-Paredes G, Beristain CI, Romero-Tehuitzil H. 2001. Effect of foaming agents on the stability, rheological properties, drying kinetics and flavor retention of tamarind foam-mats. Food Res Int 34:587–98.
Wang Z, Narsimhan G. 2004. Evolution of liquid holdup profile in a standing protein stabilized foam. J Coll Interf Sci 280:224–33.